15 December 2000

OPTICS COMMUNICATIONS

ELSEVIER

Optics Communications 186 (2000) 259–263

www.elsevier.com/locate/optcom

The influence of multiple-exposure recording on curvature pattern using multi-aperture speckle shear interferometry

Nandigana Krishna Mohan *

Applied Optics Laboratory, Department of Physics, Indian Institute of Technology, Madras 600 036, India

Received 8 June 2000; received in revised form 7 September 2000; accepted 18 October 2000

Abstract

A method based on multiple exposures in binomial mode of recording and its influence on curvature pattern is presented in this paper. Since the curvature information is obtained as a beat moiré between two sets of slope patterns, the multiple-exposure technique proposed in this paper can be implemented to sharpen the background slope fringes to enhance the visibility of the curvature fringes. © 2000 Published by Elsevier Science B.V.

Keywords: Speckle shear interferometry; Curvature measurement; Metrology

1. Introduction

Speckle shear photography and shear interferometry are the two well established methods for the measurement of spatial derivatives of the displacement components and non-destructive testing [1–4]. For plate bending problems and flexural analysis, the second order derivatives (curvature) of displacement components are required for calculating the stress components. Hence it is necessary to perform the optical differentiation of the slope data to obtain the curvature information. In speckle shear interferometry, the curvature fringes appear in the form of moiré patterns and these fringes result from the interaction between the two sets of slope patterns. Various optical techniques have been reported for the measurement of curvature [2,5–9]. Since the moiré fringe visualization is basically of an additive type, it is well known for its inherently low contrast. The visualization of moiré fringes is considerably improved either by suppressing the background slope fringes or by suitably modifying the density and orientation of the underlying slope patterns [7].

A method based on multiple exposures in binomial mode of operation, that is with the exposure timings in the ratio of 1:2:1, is reported in this paper to sharpen the underlying slope patterns in order to enhance the visibility of the curvature fringes. Further the effect of multiple exposures on slope fringes is also demonstrated. The experimental results using the conventional double exposure method as well as the proposed method are illustrated.

* Fax: +91-44-2350509.
E-mail address: nkmohan@acer.iitm.ernet.in (N.K. Mohan).

0030-4018/00/$ - see front matter © 2000 Published by Elsevier Science B.V.
PII: S0030-4018(00)01072-5

2. Optical arrangement and theory of fringe formation

Fig. 1 represents the schematic arrangement and it is same as reported earlier by Sharma et al. [5,6]. The imaging lens carries a mask containing three equi-spaced apertures along x-direction. The outer apertures A_1 and A_3 carry two identical wedge plates, while a suitable flat glass plate is mounted in front of the central aperture A_2 to compensate for the optical path. The object is illuminated normally by a collimated laser beam. The three aperture shear interferometer images contributions from three adjacent points on the object to one point in the image plane. Each of the two scattered fields is sheared with respect to the central one by an amount Δx_0. The present method of multiple-exposure shearography involves the recording of three exposures of the specimen, with the identical incremental load between the exposures on the same holographic plate in binomial mode of operation. That is the exposure timings are in the ratio of 1:2:1.

Consider that the object is in its initial state ($w_0 = 0$), and the first exposure E_1 with the exposure time t is made on a holographic plate; the exposure E_1 in terms of the exposure time t and the intensity distribution I_1 can be expressed as [2,5–8]

$$E_1 = tI_1 = tI_0[3 + 2\cos(\phi_{12} + \beta) + 2\cos(\phi_{23} + \beta) + 2\cos(\phi_{13} + 2\beta)] \quad (1)$$

where $I_0 = |a_1|^2 = |a_2|^2 = |a_3|^2$; $\phi_{12} = \phi_1 - \phi_2$, $\phi_{23} = \phi_2 - \phi_3$, $\phi_{13} = \phi_1 - \phi_3$; a's and ϕ's are the amplitudes and phases of the scattered wave fronts. $\beta = 2\pi\mu x$ is the phase introduced between the waves due to aperture separation, and it is responsible for the grating like structure in each speckle.

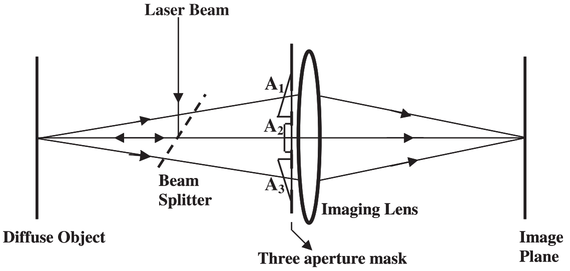

Fig. 1. Schematic of a multiple-exposure multi-aperture speckle shear interferometer.

The second exposure E_2 that represent the deformed state of the object (w_0) with the exposure time twice the exposure time of the first exposure, $2t$, is made on the same holographic plate; and E_2 can be written as

$$E_2 = 2tI_2 = 2tI_0[3 + 2\cos(\phi_{12} + \beta + \delta_{12}) + 2\cos(\phi_{23} + \beta + \delta_{23}) + 2\cos(\phi_{13} + 2\beta + \delta_{13})] \quad (2)$$

where $\delta_{12} = \delta_1 - \delta_2$, $\delta_{23} = \delta_2 - \delta_3$, $\delta_{13} = \delta_1 - \delta_3$; and δ's are the phase changes introduced by loading the object to w_0.

The object is further loaded by same amount (w_0) as given during the second exposure, and the third exposure E_3 with the exposure time t is made on the same plate. The exposure E_3 is governed by

$$E_3 = tI_3 = tI_0[3 + 2\cos(\phi_{12} + \beta + 2\delta_{12}) + 2\cos(\phi_{23} + \beta + 2\delta_{23}) + 2\cos(\phi_{13} + 2\beta + 2\delta_{13})] \quad (3)$$

where 2δ's are the phase changes introduced by equal identical loading of the object from its initial state ($2w_0$).

The total exposure E_T recorded on the holographic plate is

$$E_T = t[I_1 + 2I_2 + I_3] \quad (4)$$

When such a specklegram after processing is placed in a whole-field Fourier filtering arrangement, five halos are formed including the zeroth order at the focal plane of the lens [2]. Table 1 shows the diffraction halos and the corresponding

Table 1
Arrangement of terms in Fourier transform plane

2β	β	ZERO ORDER	$-\beta$	-2β
(A_{13})	(A_{12},A_{23})		(A_{21},A_{32})	(A_{31})
$e^{i(\phi_{13})} + 2e^{i(\phi_{13}+\delta_{13})} + e^{i(\phi_{13}+2\delta_{13})}$	$e^{i(\phi_{12})} + 2e^{i(\phi_{12}+\delta_{12})} + e^{i(\phi_{12}+2\delta_{12})} + e^{i(\phi_{23})} + 2e^{i(\phi_{23}+\delta_{23})} + e^{i(\phi_{23}+2\delta_{23})}$		$e^{i(\phi_{21})} + 2e^{i(\phi_{21}+\delta_{21})} + e^{i(\phi_{21}+2\delta_{21})} + e^{i(\phi_{32})} + 2e^{i(\phi_{32}+\delta_{32})} + e^{i(\phi_{32}+2\delta_{32})}$	$e^{i(\phi_{31})} + 2e^{i(\phi_{31}+\delta_{31})} + e^{i(\phi_{31}+2\delta_{31})}$

terms associated in these halos. Filtering through one of the first order halos gives an intensity distribution at the observation plane as

$$\begin{aligned} I_{(\text{first order})} &= |e^{i(\phi_{12})} + 2e^{i(\phi_{12}+\delta_{12})} + e^{i(\phi_{12}+2\delta_{12})} \\ &\quad + e^{i(\phi_{23})} + 2e^{i(\phi_{23}+\delta_{23})} + e^{i(\phi_{23}+2\delta_{23})}|^2 \\ &= C\Big[2\cos(\phi) + 4\cos(\phi-\delta_{12}) \\ &\quad + 4\cos(\phi+\delta_{23}) + 2\cos(\phi-2\delta_{12}) \\ &\quad + 2\cos(\phi+2\delta_{23}) \\ &\quad + 4\cos(\phi+\delta_{23}-\delta_{12}) \\ &\quad + 2\cos(\phi+\delta_{23}-2\delta_{12}) \\ &\quad + 2\cos(\phi+2\delta_{23}-\delta_{12}) \\ &\quad + 2\cos(\phi+2\delta_{23}-2\delta_{12}) \\ &\quad + 16\cos^4\frac{\delta_{12}}{2} + 16\cos^4\frac{\delta_{23}}{2}\Big] \end{aligned} \tag{5}$$

where C is a constant and $\phi = \phi_{23} - \phi_{12}$.

All the terms in the above equation containing ϕ's are random and contribute to speckle noise. The last two terms contribute to fringe formation and they are $16\cos^4(\delta_{12}/2)$ and $16\cos^4(\delta_{23}/2)$. The fringe patterns obtained by filtering via the first order halo display an intensity profile of $\cos^4$ nature, whereas in the double exposure conventional shearography it is of $\cos^2$ nature [2]. It is obvious from the intensity profile that the fringe patterns generated from the binomial mode of exposures are sharpened.

Following the analysis in Refs. [5–8], the relative phase difference between the phase terms δ_{12} and δ_{23} can be written as

$$\delta_{12} - \delta_{23} = \frac{4\pi}{\lambda}\frac{\delta^2 w}{\delta x^2}\Delta x_0^2 \tag{6}$$

The expression refers to the phase differences at two surface points whose centres are laterally shifted between themselves by a distance Δx_0.

The equation corresponding to curvature contours follows as [2,5–8]

$$\frac{\delta^2 w}{\delta x^2} = \frac{n\lambda}{2\Delta x_0^2} \tag{7}$$

The fringes depicting curvature contours appear as a moiré pattern between two sets of sharpened slope contour maps arising one each from the contribution of phase terms δ_{12} and δ_{23} respectively.

Similarly filtering through the second order halo yields the intensity distribution in the image plane as [2,5–8]

$$\begin{aligned} I_{(\text{second order})} &= |e^{i(\phi_{13})} + 2e^{i(\phi_{13}+\delta_{13})} + e^{i(\phi_{13}+2\delta_{13})}|^2 \\ &= C'\left[\cos^4\frac{\delta_{13}}{2}\right] \end{aligned} \tag{8}$$

where the phase change $\delta_{13} = \delta_{12} + \delta_{23}$ and C' is a constant.

The expression for the formation of bright fringes can be written as [2,5–8]

$$\frac{\delta w}{\delta x} = \frac{n\lambda}{4\Delta x_0} \tag{9}$$

The sharpened slope fringes in the second order halo have double the sensitivity of that in the first order.

3. Experimental results

The experiments are conducted on a centrally loaded diaphragm with its edges rigidly clamped using the conventional double exposure as well as the proposed binomial mode of three exposures, in the ratio of 1:2:1 with identical load ($W_{out} = 10$ μm) between the exposures. The diaphragm is fabricated from a phosphor bronze sheet of 0.7 mm thickness and 60 mm diameter. It is coated with an aluminium paint and the specimen is illuminated normally with a collimated beam from a 25 mW He–Ne laser. The aperture mask contains three 5 mm diameter holes with an inter spacing of 20 mm. Two wedges with 1° wedge angle are mounted on outer holes, while a glass plate of suitable thickness is mounted in front of the central hole. The aperture mask is properly mounted in front of a standard camera lens ($f = 150$ mm). The specklegrams are recorded on 10E75 holographic plates.

The fringe patterns of moiré curvature contours and slope contours obtained by Fourier filtering through first and second order halos are shown in Figs. 2 and 3 respectively. The moiré curvature fringe pattern in Fig. 2(a) corresponds to that of

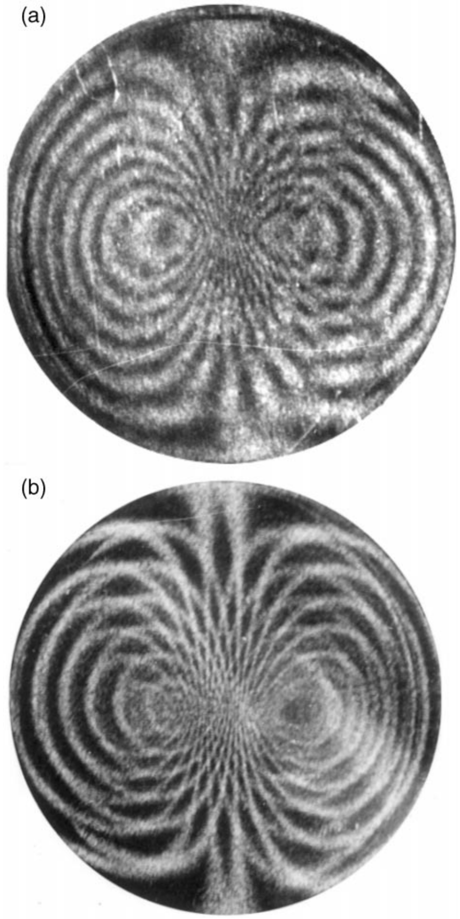

Fig. 2. Filtered curvature fringes appearing as a moiré between two slope patterns for a centrally loaded diaphragm: (a) double exposure method (1:1), (b) multiple-exposure method with the exposure timings in the ratio of 1:2:1.

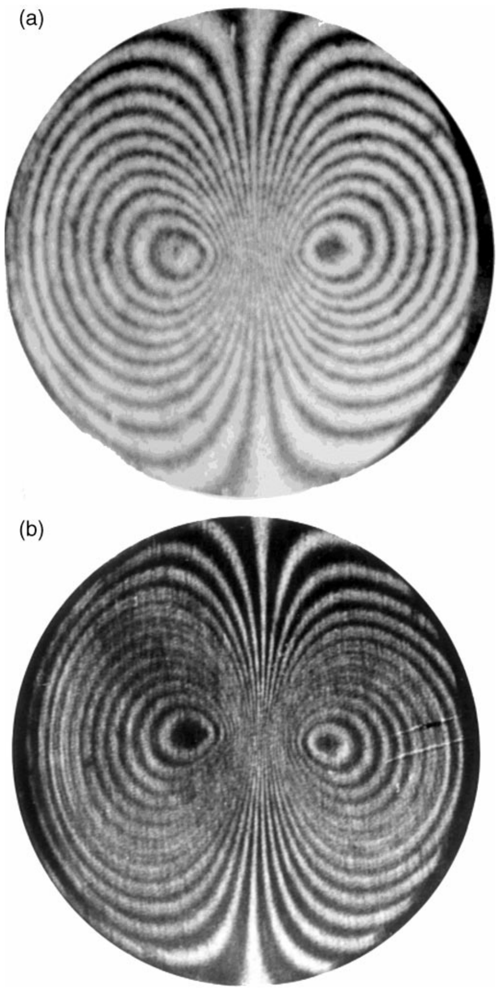

Fig. 3. Filtered slope fringes patterns for a centrally loaded diaphragm: (a) double exposure method (1:1), (b) multiple-exposure method with the exposure timings in the ratio of 1:2:1.

conventional double exposure method, where the background slope fringe profile is of the $\cos^2$ nature, while in Fig. 2(b) the curvature contours appear as a moiré between two sets of sharpened slope patterns. The fringe profile follows $\cos^4$ nature, and this results in an increase in the width of the dark slope fringes. From the photographs, it clearly shows that the visibility of moiré curvature contours in Fig. 2(b) is considerably improved by sharpening of the underlying slope patterns. Similarly Fig. 3(a) and (b) shows the filtered slope patterns obtained from double exposure and multiple-exposure methods respectively. Fig. 3 shows the slope patterns with double the sensitivity of the slope fringes appearing in Fig. 2.

4. Conclusion

The influence of multiple-exposure recording on curvature pattern using a conventional shearography arrangement is studied theoretically, and the results obtained on a central loaded diaphragm with its edges rigidly clamped are shown experimentally.

References

[1] P.K. Rastogi, Appl. Opt. 37 (1998) 1292.
[2] P.K. Rastogi, in: R.S. Sirohi (Ed.), Speckle Metrology, Marcel Dekker, New York, 1993, p. 41 (Chapter 2).
[3] Y.Y. Hung, Opt. & Lasers Eng. 29 (1998) 103.
[4] R.S. Sirohi (Ed.), Selected Papers on Speckle Metrology, SPIE Optical Engineering Press, 1991.
[5] D.K. Sharma, R.S. Sirohi, M.P. Kothiyal, Appl. Opt. 23 (1984) 1542.
[6] D.K. Sharma, N.K. Mohan, R.S. Sirohi, Opt. Commun. 57 (1986) 230.
[7] P.K. Rastogi, J. Mod. Opt. 38 (1991) 1251.
[8] C.J. Tay, S.L. Toh, H.M. Shang, Q.Y. Lin, Appl. Opt. 34 (1995) 2202.
[9] P.K. Rastogi, Opt. Lett. 21 (1996) 905.